Universal scaling of Néel temperature, staggered magnetization density, and spin-wave velocity of three-dimensional disordered and clean quantum antiferromagnets

D.-R. Tan and F.-J. Jiang*

Department of Physics, National Taiwan Normal University, 88, Sec.4, Ting-Chou Rd., Taipei 116, Taiwan

(Received 28 October 2016; revised manuscript received 28 December 2016; published 28 February 2017)

The Néel temperature, staggered magnetization density, as well as the spin-wave velocity of a three-dimensional (3D) quantum Heisenberg model with antiferromagnetic disorder (randomness) are calculated using first-principles nonperturbative quantum Monte Carlo simulations. In particular, we examine the validity of universal scaling relations that are related to these three studied physical quantities. These relations are relevant to experimental data and are firmly established for clean (regular) 3D dimerized spin-1/2 Heisenberg models. Remarkably, our numerical results show that the considered scaling relations remain true for the investigated model with the introduced disorder. In addition, while the presence of disorder may change the physical properties of regular dimerized models, hence leading to different critical theories, both the obtained data of Néel temperature and staggered magnetization density in our study are fully compatible with the expected critical behavior for clean dimerized systems. As a result, it is persuasive to conclude that the related quantum phase transitions of the considered disordered model and its clean analogues are governed by the same critical theory, which is not always the case in general. Finally, we also find smooth scaling curves even emerging when both the data of the investigated disordered model as well as its associated clean system are taken into account concurrently. This in turn implies that, while in a restricted sense, the considered scaling relations for 3D spin-1/2 antiferromagnets are indeed universal.

DOI: 10.1103/PhysRevB.95.054435

I. INTRODUCTION

Universality is an elegant concept and frequently appears in all fields of physics in various forms. In addition to being important in theoretical physics, the idea of universality can also serve as useful guidelines for experiments. One well-known example of the usefulness of universality is the critical exponents of second order phase transitions [1–3]. Specifically, the numerical values of critical exponents, such as ν related to the correlation length and β associated with the magnetization, do not in principle depend on the microscopic details of the underlying models, but are closely connected to the symmetries of the considered systems. For example, the zero temperature phase transitions of two-dimensional (2D) dimerized quantum Heisenberg models are governed by the $O(3)$ universality class [4–10], which is originally resulted from the three-dimensional (3D) classical Heisenberg model [11,12]. Furthermore, the spatial dimerization patterns have no impact on the critical theories of these quantum phase transitions (however, there may be anomalous corrections to scalings [6,10,13]). Another noticeable kind (and example) of universality is the generally applicable finite-temperature and finite-volume expressions of several physical quantities of antiferromagnets [14–28]. To be more precise, based on the corresponding low-energy effective field theory, the theoretical predictions of these observables, such as staggered and uniform susceptibilities, depend solely on a few parameters and have the same forms regardless of the magnitude of the spin of the systems. In conclusion, universality does play a crucial role in major areas of physics.

Recently, the experimental data of the phase diagram of $TlCuCl_3$ under pressure [29–31] have triggered many studies both theoretically and experimentally. In particular, several universal scaling relations are established for 3D quantum antiferromagnets [32–36]. Specifically, near the quantum phase transitions of clean (regular) 3D dimerized spin-1/2 Heisenberg models, the Néel temperatures T_N scale in several universal manners with the corresponding staggered magnetization density M_s regardless of the dimerization patterns. In addition, a quantum Monte Carlo study conducted later demonstrates that these universal scaling relations even remain valid when (certain kinds of) quenched bond disorder, i.e., antiferromagnetic bond randomness are introduced into the systems [37]. Notice the upper critical spatial dimension of the mentioned zero-temperature phase transitions is three. Consequently, close to the critical points one expects to observe multiplicative logarithmic corrections to T_N and M_s when these quantities are considered as functions of the strength of dimerization. Very recently, an analytic investigation even argues that the widely believed phase diagram of 3D quantum antiferromagnets is modified dramatically due to these logarithmic corrections [38]. The exponents related to these logarithmic corrections are determined analytically in Refs. [39–42]. Furthermore, the theoretical predictions of the numerical values of these new exponents have been verified as well [41]. Notice that the exponents related to the logarithmic corrections to T_N and M_s take the same values for three spatial dimensions. Using this result as well as the fact that the β and ν have the same mean-field values, it is straightforward to show that close the phase transition, as functions of their corresponding M_s, $T_N/c^{3/2}$, and $T_N/\overline{J}$ are linear in M_s without any logarithmic corrections. Here, c and $\overline{J}$ are the low-energy constant spin-wave velocity and the average of antiferromagnetic couplings, respectively. These connections between T_N and the associated M_s, namely $T_N/c^{3/2} = AM_s$ and $T_N/\overline{J} = A_1 M_s$ (A and A_1 are some constants) in the vicinity of a quantum critical point are confirmed in Ref. [41].

*fjjiang@ntnu.edu.tw

In real materials, impurities are often present [43]. In addition, studies of quenched disorder effects on Heisenberg-type models continue to be one of the active research topics in condensed matter physics [44]. Therefore one intriguing physics to explore further is that whether the logarithmic corrections, as well as the linear dependence of $T_N/c^{3/2}$ and T_N/J on their associated M_s are valid for 3D systems with the presence of antiferromagnetic bond disorder. Since such studies of disordered models are relevant to the experimental data of $TlCuCl_3$, in this investigation we have carried out a large-scale quantum Monte Carlo simulations of a 3D spin-1/2 antiferromagnet with configurational disorder which is first introduced in Ref. [45]. Remarkably, our data indicate convincingly that for the studied disordered model, $\overline{T_N}/\overline{c}^{3/2}$ and $\overline{T_N}/\overline{J}$ do depend on their corresponding $\overline{M_s}$ linearly close to the associated quantum phase transition (in this study observables with a overline on them refer to the results of disorder average). Furthermore, the obtained data of $\overline{T_N}$ and $\overline{M_s}$ here can be described well by the expected critical behavior for regular dimerized models. This suggests that the related quantum phase transition of the considered disordered system may be governed by the same critical theory as that of its clean analogues. It should be pointed out that while close to the considered quantum critical point the relations $\overline{T_N}/\overline{c}^{3/2} = A\overline{M_s}$ and $\overline{T_N}/\overline{J} = A_1\overline{M_s}$ hold even for the investigated model with the employed disorder, based on the results of current and previous studies, we find that the prefactors A and A_1 are likely to be model-dependent. Surprisingly, when both the data of current study and that of a clean system available in Ref. [35] are taken into account concurrently, smooth universal curves appear. This in turn implies that, while in a restricted sense, the investigated scaling relations of 3D spin-1/2 antiferromagnets are indeed universal. Finally, although the prefactor A of $T_N/c^{3/2} = AM_s$ ($\overline{T_N}/\overline{c}^{3/2} = A\overline{M_s}$) is likely not universal, we find the quantity $A/(J'/J)_c^{3/2}$, where $(J'/J)_c$ is the considered critical point, obtained in this study matching very well with the corresponding one in Ref. [41]. This indicates that with an appropriate normalization, a true universal quantity may still exist.

This paper is organized as follows. After the introduction, in Sec. II, we define the investigated model as well as the calculated observables. We then present a detail analysis of our numerical data in Sec. III. In particular, the scaling relation $T_N/c^{3/2} = AM_s$ as well as the logarithmic corrections to T_N and M_s are examined carefully. Finally, in Sec. IV, we conclude our study.

II. MICROSCOPIC MODEL, CONFIGURATIONAL DISORDER, AND OBSERVABLES

The 3D quantum Heisenberg model with random antiferromagnetic couplings studied here is given by the Hamilton operator

$$H = \sum_{\langle ij\rangle} J_{ij}\,\vec{S}_i\cdot\vec{S}_j + \sum_{\langle i'j'\rangle} J'_{i'j'}\,\vec{S}_i\cdot\vec{S}_j, \tag{1}$$

where J_{ij} and $J'_{i'j'}$ are the antiferromagnetic couplings (bonds) connecting nearest neighbor spins $\langle ij\rangle$ and $\langle i'j'\rangle$, respectively, and $\vec{S}_i$ is the spin-1/2 operator at site i. The bond disorder

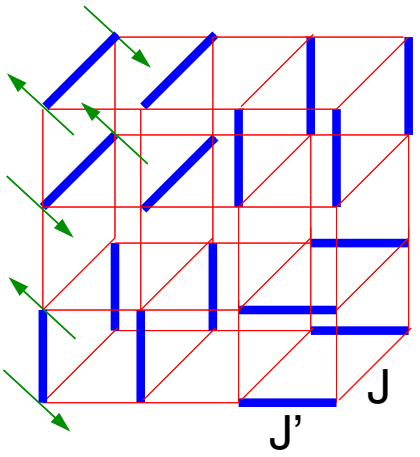

FIG. 1. The model with configurational disorder studied here.

considered in this investigation is a generalization of the configurational disorder introduced in Ref. [45] and is realized here as follows. First of all, a given cubical lattice is subdivided into two by two by two cubes. Secondly, the 12 bonds within a cube are classified into three sets of bonds so that each of them is made up of four bonds parallel to a particular coordinate axis. Furthermore, one of the three sets of bonds of every cube is chosen randomly and uniformly. In particular, these picked bonds are assigned the antiferromagnetic coupling strength J'. Finally, the remaining unchosen bonds as well as those not within any cubes have antiferromagnetic coupling strength J, which is set to be 1.0 in this investigation. Figure 1 demonstrates one realization of the model with configurational disorder studied here. Notice in our study the couplings J' and J satisfy $J' > J$. Hence as the ratio of J'/J increases, the system will undergo a quantum phase transition.

To determine the Néel temperature $\overline{T_N}$, the staggered magnetization density $\overline{M_s}$, as well as the spin-wave velocity $\overline{c}$ of the considered models with the employed configurational disorder, the observables staggered structure factor $\overline{S(\pi,\pi)}$, both the spatial and temporal winding numbers squared ($\overline{\langle W_i^2\rangle}$ for $i \in \{1,2,3\}$ and $\overline{\langle W_t^2\rangle}$), spin stiffness $\overline{\rho_s}$, first Binder ratio $\overline{Q_1}$, and second Binder ratio $\overline{Q_2}$ are calculated in our simulations. The quantity $\overline{S(\pi,\pi)}$ takes the form

$$\overline{S(\pi,\pi)} = 3\overline{\langle (m_s^z)^2\rangle} \tag{2}$$

on a finite cubical lattice with linear size L. Here, $m_s^z = \frac{1}{L^3}\sum_i (-1)^{i_1+i_2+i_3} S_i^z$ with S_i^z being the third-component of the spin-1/2 operator $\vec{S}_i$ at site i. In addition, the spin stiffness $\overline{\rho_s}$ has the following expression:

$$\overline{\rho_s} = \frac{1}{3\beta L}\sum_{i=1,2,3}\overline{\langle W_i^2\rangle}, \tag{3}$$

where β is the inverse temperature. Finally, the observables $\overline{Q_1}$ and $\overline{Q_2}$ are defined by

$$\overline{Q_1} = \frac{\overline{\langle |m_s^z|\rangle^2}}{\overline{\langle (m_s^z)^2\rangle}} \tag{4}$$

and

$$\overline{Q_2} = \frac{\overline{\left\langle \left(m_s^z\right)^2 \right\rangle}^2}{\overline{\left\langle \left(m_s^z\right)^4 \right\rangle}}, \tag{5}$$

respectively. With these observables, the physical quantities required for our study, namely $\overline{T_N}$, $\overline{M_s}$, and $\overline{c}$, can be calculated accurately.

III. THE NUMERICAL RESULTS

To examine whether the scaling relations $\overline{T_N}/\overline{c}^{3/2} = A\overline{M_s}$ and $\overline{T_N}/\overline{J} = A_1\overline{M_s}$, where A and A_1 are some constant, appear for the considered 3D quantum Heisenberg models with the introduced configurational disorder, we have carried out a large-scale Monte Carlo simulation using the stochastic series expansion (SSE) algorithm with very efficient loop-operator update [46]. We also use the β-doubling scheme [47] in our simulations so that $\overline{M_s}$ can be obtained efficiently. Here, β refers to the inverse temperature. Specifically the β-doubling scheme works as follows [48]. First of all, each generated disordered configuration is simulated with inverse temperatures $\beta = 2^n, n = 0,1,2,3,4,5,\ldots,n_{\max}$ sequentially. Furthermore, for every fixed $\beta = 2^i$, one carries out simulations with N Monte Carlo steps for thermalization (without performing the measurement). Here, one Monte Carlo step consists of one diagonal update, one loop update, and flipping each free spin with probability 1/2. Following this one additionally executes $2N$ Monte Carlo steps with measurements for the same $\beta = 2^i$. This N–$2N$ procedure is done two times before moving to the calculations of $\beta = 2^{i+1}$. Notice prior to starting the simulations for $\beta = 2^{i+1}$, i.e., performing the N–$2N$ procedure at $\beta = 2^{i+1}$, the (number of) operators including the identity operator in the last operator sequence S_M (SSE sequence) associated with $\beta = 2^i$ is doubled from M to $2M$, resulting in a new operator sequence S_{2M} which will be used as the initial configuration for the calculations at $\beta = 2^{i+1}$. In the initial SSE sequence S_{2M} of the simulations for $\beta = 2^{i+1}$, the first M operators are the same as the ones of S_M. Moreover, the second set of M operators in S_{2M}, namely the $(M+1)$th to $2M$th operators are exact copy of those of the first M operators, either in the same order or reversed order. These described procedures are repeated until the calculations for $\beta = 2^{n_{\max}}$ are finished.

Notice the convergence of the considered observables to their ground state values is reached when the disorder-averaged results from the last four consecutive measurements, namely the measurements carried out at $\beta = 2^{n_{\max}}$ and $\beta = 2^{n_{\max}-1}$, are consistent quantitatively with each other. Furthermore, the consistency between the two successive measurements done at the same β in the disordered average indicates that the errors related to equilibration (thermalization), at least for the second measurement, is smaller than the statistical errors. Hence in the production simulations, ideally one has to make sure that the $n_{\max}$, as well as the Monte Carlo steps N in the N–$2N$ procedure introduced above, should be large so that the zero temperature results are obtained and the thermalization is reached for all temperatures. We would like to emphasize the fact that with the β-doubling scheme, the starting operator sequences for lower temperatures should be in general not far away from being thermalized. As a result, this method is very efficient for studying the ground state properties of disordered systems.

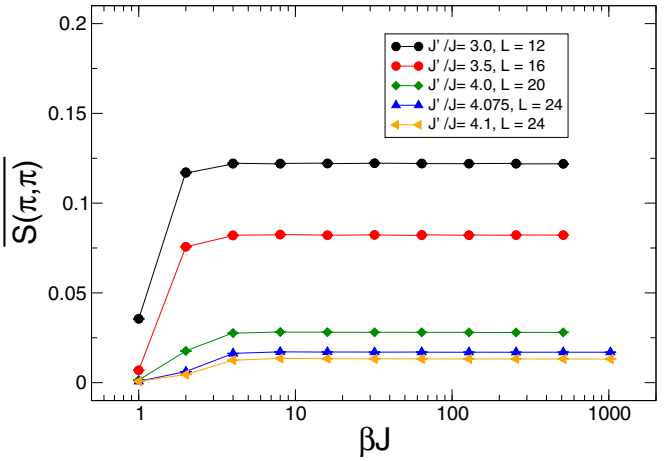

FIG. 2. Convergence of the structure factors $\overline{S(\pi,\pi)}$ to their ground-state values for several considered J'/J and box sizes L. The solid lines are added to guide the eye.

It should be pointed out that each disordered configuration in this study is generated by its own random seed in order to reduce the effect of correlation between observables determined from different configurations. Our preliminary results indicate that the critical point $(J'/J)_c$ lies between 4.15 and 4.17. Hence we have focused on the data of $J'/J \leqslant 4.13$. Notice in our study, $\overline{M_s}$ are calculated using several hundred configurations and $\overline{T_N}$ ($\overline{c}$) are determined with several thousand (few to several ten thousand) disorder realizations. The convergence of the considered observables to their correct values associated with the employed disorder, as well as the systematic uncertainties due to Monte Carlo sweeps within each randomness realization, number of configurations used for disorder average, and thermalization are examined by performing many trial simulations and analysis. The resulting data from these trial simulations and analysis agree quantitatively with those presented here. Notice the statistics reached for studies of clean systems typically are better than those of investigation related to disordered models. Therefore we have additionally carried out many calculations using exactly the same parameters to estimate the uncertainties due to the statistics obtained here. In summary, the quoted errors of the calculated observables in this study are estimated with conservation so that the influence of these mentioned potential systematic uncertainties are not underestimated.

A. The determination of $\overline{M_s}$

The observable considered here for the calculations of $\overline{M_s}$ is $\overline{S(\pi,\pi)}$. Specifically, for a given J'/J, the related $\overline{M_s}$ is given by the square root of the corresponding bulk $\overline{S(\pi,\pi)}$. It should be pointed out that the zero temperature, namely the ground state values of $\overline{S(\pi,\pi)}$ are needed for these calculations. Hence the β-doubling scheme is used here. The β dependence, i.e., inverse temperature-dependence of $\overline{S(\pi,\pi)}$ for several considered J'/J and L is shown in Fig. 2. In addition, the $1/L$ dependence of the ground-state $\overline{S(\pi,\pi)}$ for

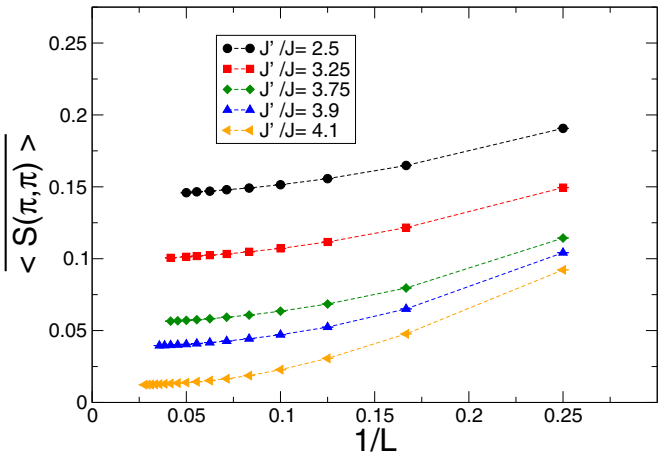

FIG. 3. $1/L$ dependence of the staggered structure factors $\overline{S(\pi,\pi)}$ for several considered values of J'/J. The dashed lines are added to guide the eye.

some studied J'/J is depicted in Fig. 3. The largest box size reached here for calculating the staggered structure factors is $L = 36$. Motivated by the theoretical predictions in Ref. [49], the determination of $\overline{M_s}$ is done by extrapolating the related finite volume staggered structure factors to the corresponding bulk results, using the following four *Ansätze*:

$$a_0 + a_1/L + a_2/L^2 + a_3/L^3, \tag{6}$$

$$b_0 + b_1/L + b_2/L^2, \tag{7}$$

$$c_0 + c_2/L^2 + c_3/L^3, \tag{8}$$

$$d_0 + d_2/L^2. \tag{9}$$

In particular, the $\overline{M_s}$ corresponding to each (good) fit is obtained by taking the square root of the resulting constant term. The numerical values of $\overline{M_s}$ determined from the fits employing *Ansätze* (6), (7), and (8) are shown in Fig. 4. For most considered J'/J, the $\overline{M_s}$ obtained from the fits using

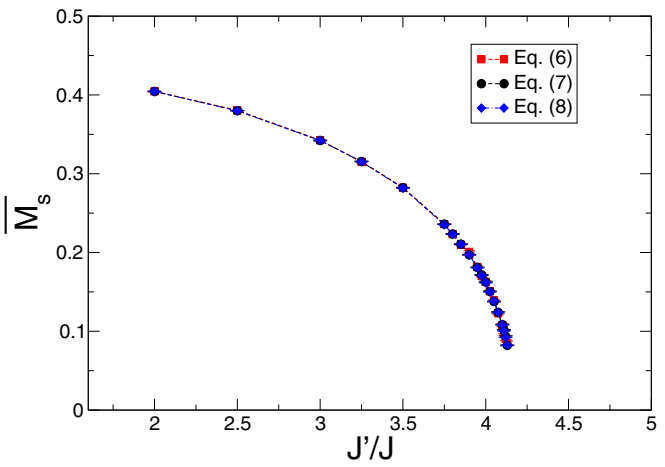

FIG. 4. $\overline{M_s}$ as functions of the considered values of J'/J. The dashed lines are added to guide the eye.

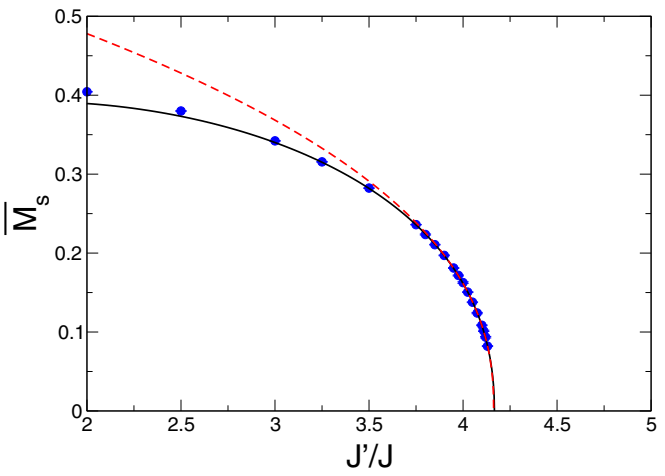

FIG. 5. Fits of $\overline{M_s}$ to the *Ansatz* of Eq. (10) (solid line) and a pure power function $a_1|j_c - j|^{b_1}$ (dashed line). The range of J'/J and χ^2/DOF for the fit using Eq. (10) (*Ansatz* $a_1|j_c - j|^{b_1}$) are $J'/J \geqslant 3.75$ and 1.2 ($J'/J \geqslant 3.9$ and 1.1), respectively. The leading exponent b of Eq. (10) (b_1 of $a_1|j_c - j|^{b_1}$) determined from the fit is 0.513(6) (0.42(1)). Applying the *Ansatz* $a_1|j_c - j|^{b_1}$ [Eq. (10)] to fit the data containing those of $J'/J \leqslant 3.5$ ($J'/J \leqslant 2.5$) leads to very poor fitting quality.

these three *Ansätze* match each other very well. For the few cases where the agreement between the three results of $\overline{M_s}$ is not satisfactory, we find that the ones computed from the fits associated with *Ansatz* (7) are consistent with those obtained by applying either *Ansatz* (6) or *Ansatz* (8) to fit the data. Therefore the $\overline{M_s}$ resulting from the analysis using *Ansatz* (7) are used for the required investigation in the following. Occasionally, *Ansatz* (9) is considered for consistency check as well.

In Ref. [41], the 3D dimerized double cubic quantum Heisenberg model is studied. In particular, the relation of $T_N/c^{3/2} = AM_s$ is examined in detail. Since three spatial dimensions is the upper critical dimension of the quantum phase transition considered in Ref. [41], one expects to observe logarithmic corrections to M_s and T_N when approaching the critical point. The theoretical calculations of the critical exponents associated with these logarithmic corrections are available in Refs. [39–41], and the predicted values are confirmed by a careful analysis of M_s and T_N conducted in Ref. [41]. Since disorder may change the upper critical dimension of the clean system, it will be interesting to check whether this is indeed the case for our model. The exponent related to the logarithmic correction to M_s, namely $\hat{\beta}$ has a value of $\frac{3}{11}$ for 3D clean dimerized model. Inspired by this, we have fitted our $\overline{M_s}$ data to an *Ansatz* of the form

$$a|j_c - j|^b |\ln(|(j_c - j)/j_c|)|^{3/11}, \tag{10}$$

where $j = J'/J$ [$j_c = (J'/J)_c$ is the critical point] and a is a constant. Notice the b appearing in Eq. (10) is the associated leading critical exponent, which is predicted to be 0.5. Interestingly, we find that the numerical values of b [in Eq. (10)] obtained from the fits have an average of 0.507(18), which is in reasonably good agreement with the predicted mean-field result 0.5 (see Fig. 5 for one of such fitting results).

In other words, our $\overline{M_s}$ data are consistent with the standard scenario for clean systems. This implies that the upper critical dimension of the clean model is not affected by the considered configurational disorder.

We would like to point out that the $\overline{M_s}$ data obtained here can also be fitted to the *Ansatz* $a_1|j_c - j|^{b_1}$. Furthermore, the average value of b_1 determined from the corresponding good fits is 0.410(16). Finally, the critical points $(J'/J)_c$ obtained from the fits of these two *Ansätze* are given by 4.166(3) and 4.162(3) on average, respectively. Based on these results, at this stage, we are not able to reach a definite answer of whether the calculated $\overline{M_s}$ data here receive any logarithmic correction. Later, when discussing the determination of $\overline{T_N}$, we will argue that our data are in favor of the scenario that logarithmic corrections do enter the J'/J dependence of the related observables.

B. The determination of $\overline{T_N}$

The employed observables for calculating $\overline{T_N}$ are $\overline{\rho_s}L$, $\overline{Q_1}$, as well as $\overline{Q_2}$. Notice a constraint standard finite-size scaling *Ansatz* of the form $(1 + b_0 L^{-\omega})[b_1 + b_2 t L^{1/\nu} + b_3 (t L^{1/\nu})^2 + \ldots]$, up to second, third, and (or) fourth order in $tL^{1/\nu}$, is adopted to fit the data. Here, b_i for $i = 0,1,2,\ldots$ are some constants and $t = \frac{T-\overline{T_N}}{\overline{T_N}}$. For some J'/J, *Ansatz* up to fifth order in $tL^{1/\nu}$ is used. The data of $\overline{\rho_s}L$ and $\overline{Q_2}$ for $J'/J = 2.0$ ($J'/J = 3.0$) are shown in Fig. 6 (Fig. 7). In addition, the $\overline{Q_1}$ data of $J'/J = 3.8$ and $J'/J = 3.95$ are presented in Fig. 8. For every J'/J, *Ansätze* of various orders in $tL^{1/\nu}$ are employed to fit several sets of data (each set of data has different range of L). The cited values of $\overline{T_N}$ in this study are estimated by averaging the corresponding results of good fits. Furthermore, the error bar of each quoted $\overline{T_N}$ is determined from the uncertainty of every individual $\overline{T_N}$ of the associated good fits. For this analysis, we consider a fit with $\chi^2/\mathrm{DOF} \lessapprox 2.0$ a good fit. In some cases, more restricted conditions on χ^2/DOF and the obtained results are imposed for consistency. The determined $\overline{T_N}$ from the observables $\overline{\rho_s}L$, $\overline{Q_1}$, and $\overline{Q_2}$ are shown in Fig. 9 [50]. In addition to $\overline{T_N}$, other interesting physical quantities to study are the critical exponents ν and ω appearing in the relevant finite-size scaling *Ansätze* . Notice the dimensionality as well as some critical exponents are present in the conventional finite-size scaling *Ansatz* involving ρ_s. Based on the analysis of $\overline{M_s}$ in previous section, while it is plausible to employ the conventional finite-size scaling *Ansatz* of clean models for the considered finite-temperature phase transitions, one cannot rule out the possibility that when J'/J is close enough to the critical point, the effective dimensions of the systems as well as the values of the exponents in the scaling *Ansatz* receive corrections due to the employed disorder. On the other hand, because of their definition, Binder ratios, like $\overline{Q_1}$ and $\overline{Q_2}$ calculated here, do not encounter such kind of subtlety. Indeed, the values of ν obtained from the fits related to $\overline{\rho_s}L$ are systematic smaller than the corresponding results associated with $\overline{Q_1}$ and $\overline{Q_2}$. Such a trend is becoming more clear as one approaches the quantum critical point $(J'/J)_c$. Hence here we only summarize the results of ν obtained from fitting the data of $\overline{Q_1}$ and $\overline{Q_2}$ to their expected *Ansätze* [51]. The individual average ν of J'/J with $J'/J < 4.0$, obtained

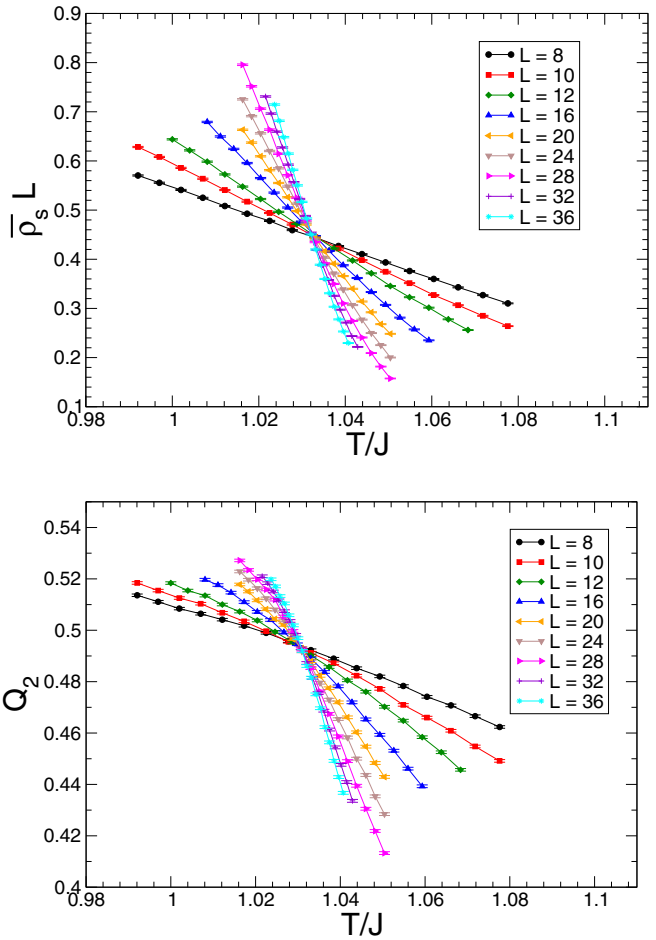

FIG. 6. $\overline{\rho_s}L$ (top) and $\overline{Q_2}$ (bottom) as functions of T/J for $J'/J = 2.0$ and $L = 8$, 10, 12, 16, 20, 24, 28, 32, and 36. J is 1.0 in our calculations. The solid lines are added to guide the eye.

from the related good fits of $\overline{Q_1}$ ($\overline{Q_2}$), range from 0.69 to 0.72 (0.69 to 0.73). On the other hand, the values of ν calculated for $4.0 \leqslant J'/J \leqslant 4.12$ ($J'/J = 4.13$) lie between 0.63 and 0.69 (0.60 and 0.62). We attribute this result to the fact that data of large box size are limited for $J'/J \geqslant 4.0$. Such scenario is observed for clean dimerized models as well [6,10]. Finally, the determination of ω with reasonable precision is hindered by the strong correlation between ω and its related prefactor b_0 in the fitting formulas.

After obtaining the numerical values of $\overline{T_N}$, we turn to the study of whether a logarithmic correction, like the one associated with $\overline{M_s}$, exists for $\overline{T_N}$ when $\overline{T_N}$ is treated as a function of J'/J. Similar to our earlier analysis for $\overline{M_s}$, we use two *Ansätze*, namely,

$$a_2|j_c - j|^{b_2} \quad \text{and}$$
$$a_3|j_c - j|^{b_3}|\ln(|(j_c - j)/j_c|)|^{3/11} \tag{11}$$

to fit the data of $\overline{T_N}/\overline{J}$ determined from all the calculated observables $\overline{Q_1}$, $\overline{Q_2}$, and $\overline{\rho}_s L$. The exponent b_3 of the second *Ansatz* of Eq. (11) is predicted to take its mean-field value 0.5. Furthermore, the number 3/11 appearing above is the expected theoretical value for the exponent $\hat{\tau}$ associated with this logarithmic correction. Notice we investigate the physical

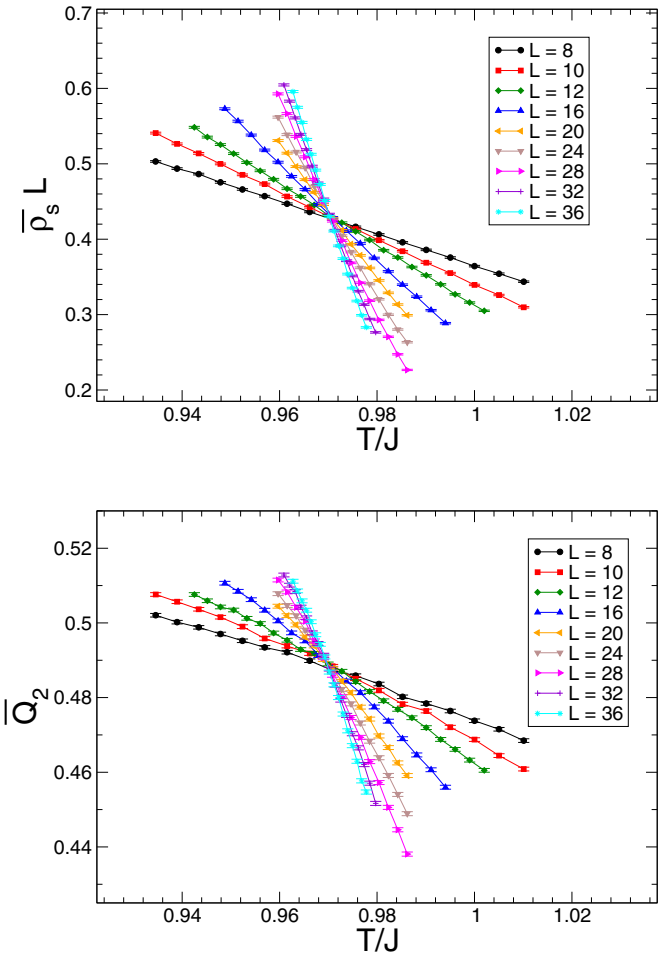

FIG. 7. $\overline{\rho_s}L$ (top) and $\overline{Q_2}$ (bottom) as functions of T/J for $J'/J = 3.0$ and $L = 8$, 10, 12, 16, 20, 24, 28, 32, and 36. J is 1.0 in our calculations. The solid lines are added to guide the eye.

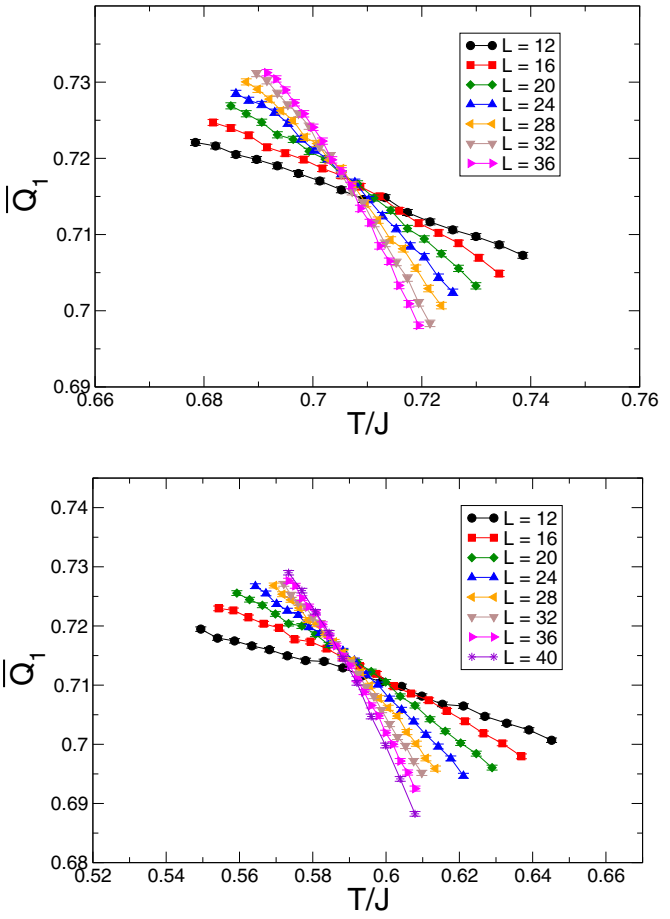

FIG. 8. $\overline{Q_1}$ as functions of T/J for $J'/J = 3.8$ (top) and $J'/J = 3.95$ (bottom). The box sizes L for these two values of J'/J are $L = 8$, 10, 12, 16, 20, 24, 28, 32, and 36 (and 40 for $J'/J = 3.95$). J is 1.0 in our calculations. The solid lines are added to guide the eye.

quantity $\overline{T_N}/\overline{J}$ instead of $\overline{T_N}$. This is motivated by the analysis done in [41]. The consideration of $\overline{T_N}/\overline{J}$ is also natural since it is a dimensionless quantity. Interestingly, for all three data sets, we arrive at good fits (χ^2/DOF $\leqslant 1.0$) using the second *Ansatz* of Eq. (11) when data points of $\overline{T_N}/\overline{J}$ with $J'/J \geqslant 3.75$ are included in the fits. On the other hand, the results obtained from applying the first *Ansatz* to fit the data have much worse fitting quality. As fewer data are included in the fits, while the results related to the second *Ansatz* remain good, the χ^2/DOF associated with the fits employing the first *Ansatz* continue to be very large (except those of the fits using data sets close to $(J'/J)_c$). Notice occasionally fits with the first *Ansatz* lead to good results, but not in a systematic manner. The exponent b_3 and the critical point $(J'/J)_c$ obtained from all the good fits are given by 0.49(1) and 4.166(2) on the average, respectively. The calculated value of b_3, namely $b_3 = 0.49(1)$ is in reasonably good agreement with the expected mean-field result 0.5. A fit of this analysis including the logarithmic correction is shown in Fig. 10. According to what has been reached so far, we conclude that our data are fully compatible with the scenario that the upper critical dimension (D_c), associated with the relevant quantum phase transition of our model, is the same as that of the corresponding clean model. In particular, the related critical exponents are in agreement with the theoretical predictions of clean systems.

For the analysis conducted above, the exponents $\hat{\beta}$ and $\hat{\tau}$ are fixed to their theoretical values for pure systems. Furthermore, the corresponding leading exponents, namely β and ν obtained

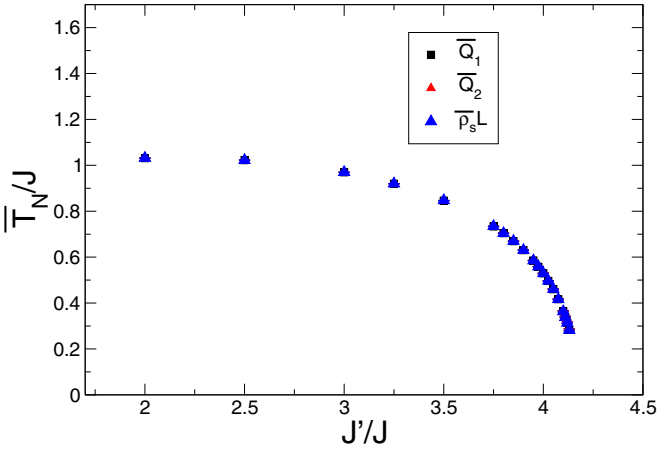

FIG. 9. $\overline{T_N}$, obtained from $\overline{Q_1}$, $\overline{Q_2}$, and $\overline{\rho_s}L$, as functions of J'/J.

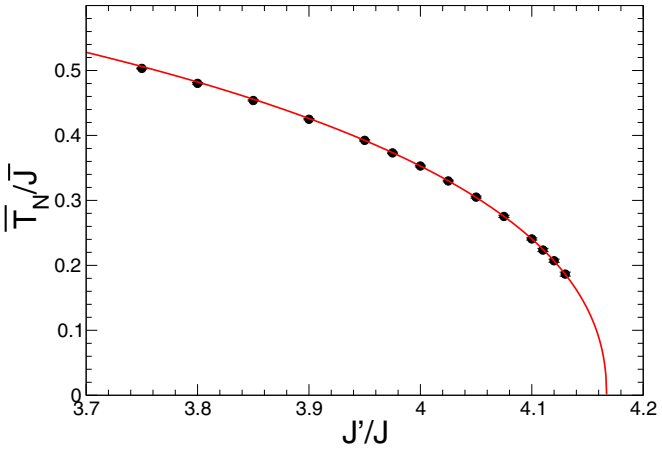

FIG. 10. Fit of $\overline{T_N}/\overline{J}$ data (obtained from $\overline{Q_1}$) with $J'/J \geqslant 4.0$ to their theoretical expression with a logarithmic correction $a_3|j_c - j|^{b_3}|\ln(|(j_c - j)/j_c|)|^{3/11}$. The b_3 obtained from the fit is given by 0.494(8). No fits using the *Ansatz* of $a_2|j_c - j|^{b_2}$ are shown because the majority of such fits are of poor quality.

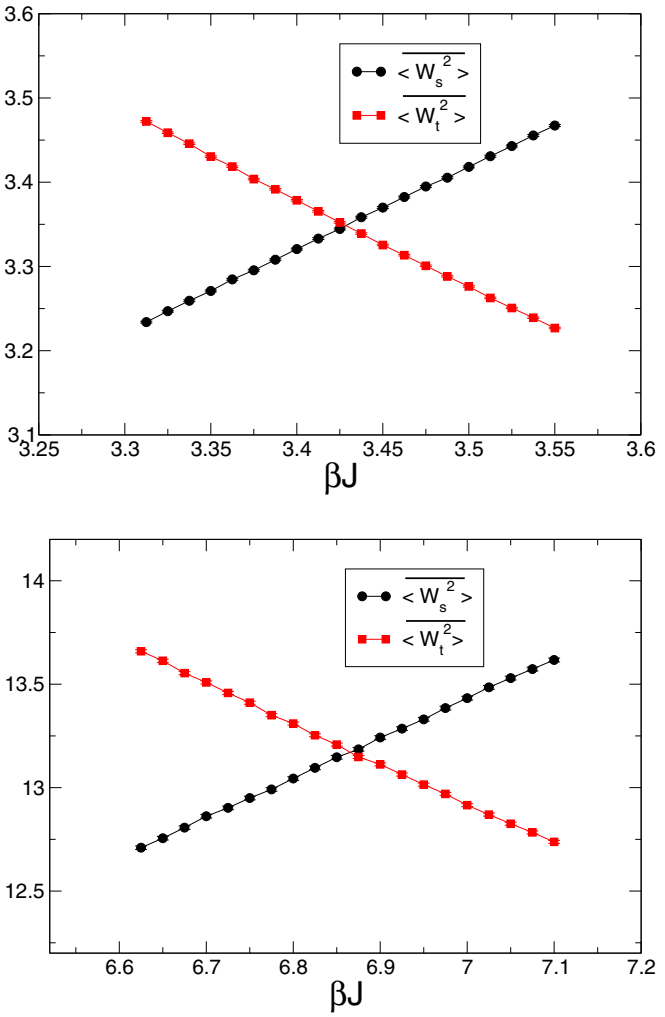

FIG. 11. The spatial and temporal winding numbers squared, as functions of βJ at $J'/J = 3.0$, for $L = 8$ (top) and 16 (bottom). J is 1.0 in our simulations.

from the fits agree nicely with those associated with clean models. One may wonder if consistent results with those of pure systems can be reached when $\hat{\beta}$ and $\hat{\tau}$ are left as free parameters in the fits. To examine whether one can arrive at such conclusions, we have carried out fits with β and ν being set to 0.5. In addition, the T_c appearing in the *Ansätze* are fixed to the ones determined in previous analysis and $\hat{\beta}$ and $\hat{\tau}$ are left as free parameters for the fits. The $\hat{\beta}$ and $\hat{\tau}$ obtained from these new fits are given by 0.245 and 0.305 in the average, respectively. The uncertainty for each individual result used for the average ranges from few percent to around ten percent. We find that the determined values of $\hat{\beta}$ ($\hat{\tau}$) are slightly smaller (larger) than 0.2727 systematically. This result reflects the fact that the β (ν) obtained from our previous analysis is a little bit greater (less) than 0.5. Notice $\hat{\beta}$ and $\hat{\tau}$ are associated with the corrections to scaling. As a result, to reach a good estimate of their numerical values requires high precision data, and in particular, data close to the critical point may be needed as well. Indeed, our analysis implies that two percent deviation from 0.5 in β (ν) leads to around 10% discrepancy from 0.2727 in $\hat{\beta}$ ($\hat{\tau}$). Considering the challenge of calculating these two quantities accurately for disordered systems, the numerical evidence we have obtained for claiming that the $\hat{\beta}$ and $\hat{\tau}$ determined here are in reasonable agreement with their predicted values of clean systems is acceptable. Interestingly, the average of the calculated $\hat{\beta}$ and $\hat{\tau}$ is 0.2750 which nicely matches the expected 0.2727 for both $\hat{\beta}$ and $\hat{\tau}$ of the related 3D pure models. In summary, our conclusion that the considered phase transition of the studied disordered model is governed by the same critical theory as that of its clean counterpart(s) is beyond reasonable doubt.

C. The determination of $\overline{c}$

The values of spin-wave velocity $\overline{c}$ are estimated using the idea of winding numbers squared as suggested in Refs. [52,53]. Specifically, for a given J'/J and a box size L, one varies the inverse temperature β so that the spatial and temporal winding numbers squared ($\overline{\langle W_s^2\rangle} = \frac{1}{3}(\overline{\langle W_1^2\rangle + \langle W_2^2\rangle + \langle W_3^2\rangle}$ and $\overline{\langle W_t^2\rangle}$) take the same values. Assuming one reaches the condition $\overline{\langle W_s^2\rangle} = \overline{\langle W_t^2\rangle}$ at an inverse temperature $\beta^\star$, then the spin-wave velocity $\overline{c}(J'/J, L)$ corresponding to this set of parameters J'/J and L is given by $\overline{c}(J'/J, L) = L/\beta^\star$. Notice with our implementation of configurational disorder, the three spatial winding numbers squared take the same values after one carries out the disorder average. For the J'/J of smaller magnitude, the convergence of $\overline{c}$ to their infinite volume values are checked using the data of $L = 8$ and 16. In addition, the bulk $\overline{c}$ for large magnitude J'/J are obtained from the data of $L = 12$ and 24. With the statistics reached here, we find that for all the considered J'/J the corresponding bulk spin-wave velocities $\overline{c}$ can be correctly given by the results at $L = 16$ or 24. The convergence of the spin-wave wave velocities to their bulk values for $J'/J = 3.0$ and 3.9 are demonstrated in Figs. 11 and 12, respectively, and the bulk $\overline{c}$ we obtained are presented in Fig. 13. We would like to point out that for $J'/J \geqslant 4.0$, our estimated central values of $\overline{c}$ for $L = 12$ and 24 differ by only less than 0.34 percent and are within their

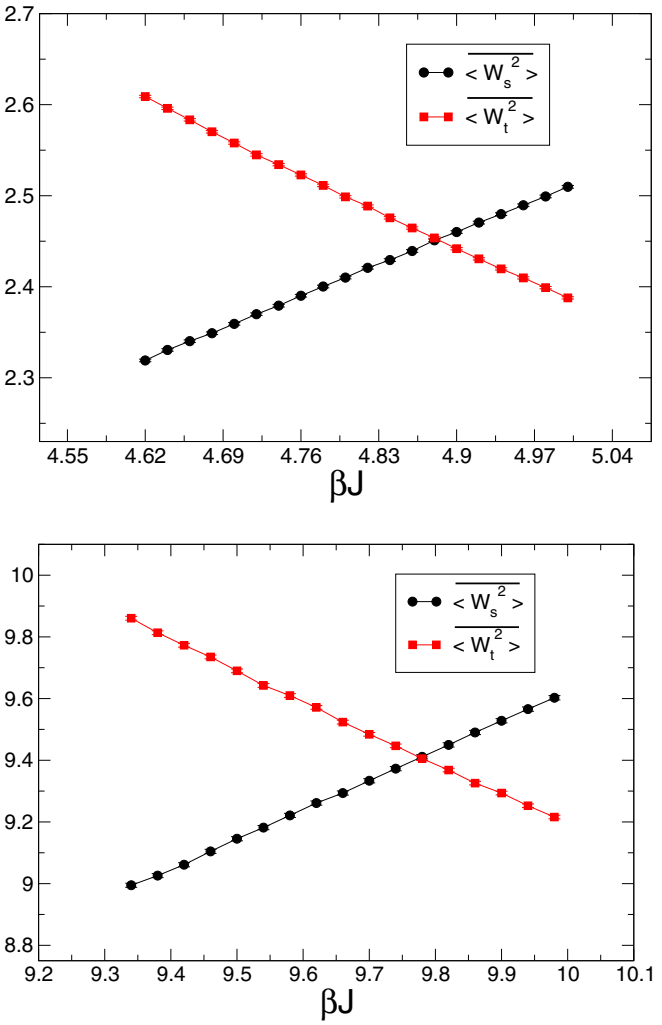

FIG. 12. The spatial and temporal winding numbers squared, as functions of βJ at $J'/J = 3.9$, for $L = 12$ (top) and 24 (bottom). J is 1.0 in our simulations.

corresponding error bars. Therefore the results of $\overline{c}$ shown in Fig. 13 should be very reliable.

D. The scaling relations $\overline{T_N}/\overline{c}^{3/2} = A\overline{M_s}$ and $\overline{T_N}/\overline{J} = A_1\overline{M_s}$

Having obtained $\overline{M_s}$, $\overline{T_N}$, and $\overline{c}$, we move to examine whether the scaling relations $\overline{T_N}/\overline{c}^{3/2} = A\overline{M_s}$ and $\overline{T_N}/\overline{J} = A_1\overline{M_s}$, which are confirmed for clean system(s), remain true for the model with the introduced configurational disorder studied here. Actually, the validity of these relations for our model is expected, since our data of $\overline{T_N}/\overline{J}$ and $\overline{M_s}$ are fully compatible with the theoretical predictions for clean systems, and neither $\overline{c}$ nor $\overline{J}$ receives any logarithmic corrections. Indeed, the obtained results of $\overline{T_N}/\overline{c}^{3/2}$, when being treated as a function of $\overline{M_s}$, can be fitted to the *Ansatz* of $A\overline{M_s}$ using the data with the corresponding $\overline{M_s}$ having small magnitude. Furthermore, the prefactor A determined from the fits has an average $A_{\rm avg} \sim 0.858(4)$. Two outcomes of the fits are demonstrated in Fig. 14. Notice both the uncertainties of $\overline{T_N}/\overline{c}$ and $\overline{M_s}$ are taken into account in the fits. Similarly, close to the

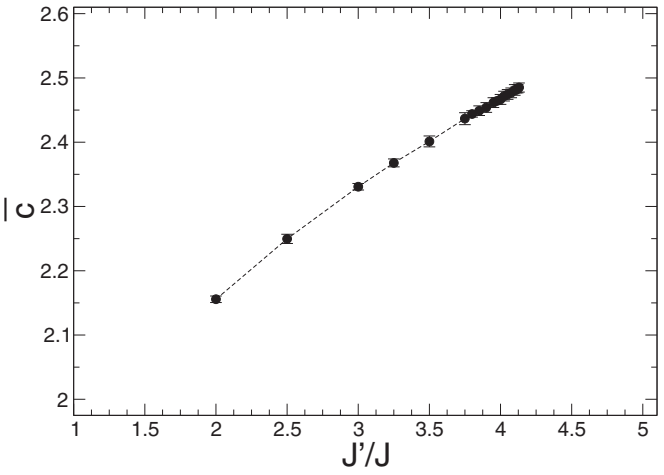

FIG. 13. The estimated values of $\overline{c}$ for all the considered J'/J.

quantum phase transition, our data of $\overline{T_N}/\overline{J}$ and $\overline{M_s}$ do satisfy a linear relation as well, see Fig. 15.

One may wonder whether the data of $\overline{T_N}/\overline{c}^{3/2}$ can be fitted to the Ansätz of the form $A\overline{M_s} + B$ with B being consistent with zero. We have applied such analyses to the data obtained

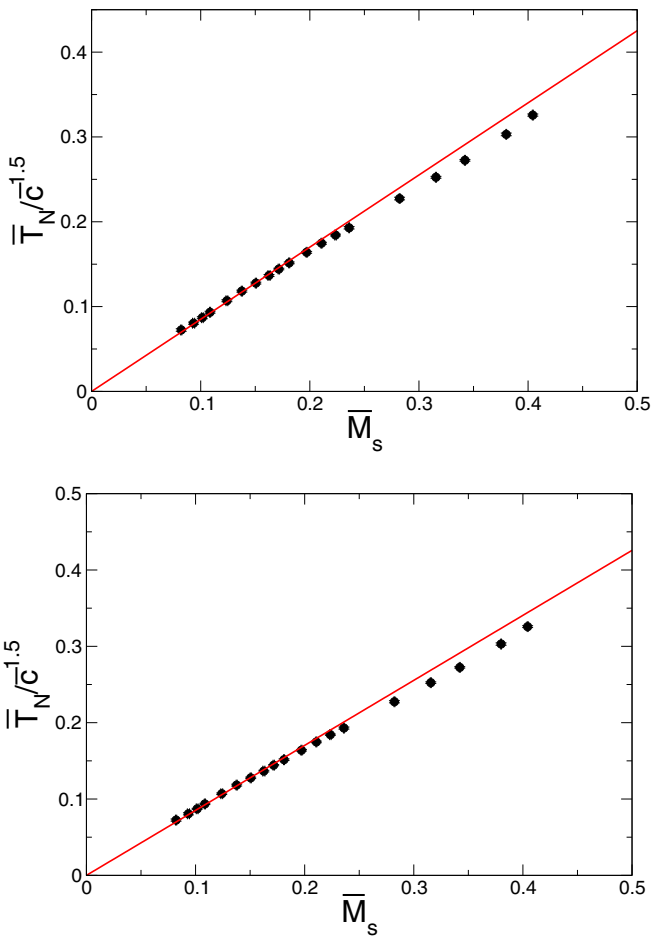

FIG. 14. Fits of $\overline{T_N}/\overline{c}^{3/2}$ as linear functions of $\overline{M_s}$ passing through the origin. The $\overline{T_N}$ of the top and bottom panels are obtained from $\overline{Q_1}$ and $\overline{Q_2}$, respectively.

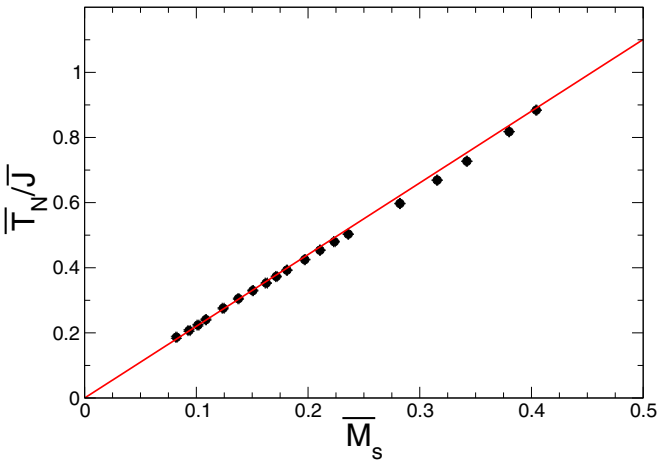

FIG. 15. Fit of $\overline{T_N}/\overline{J}$ as a linear function of $\overline{M_s}$ passing through the origin. The used values of $\overline{T_N}$ are obtained from $\overline{Q_1}$. The average of the slopes for all the good fits including those resulting from $\overline{Q_2}$ and $\overline{\rho_s}L$ is given by 2.22(1).

close to $(J'/J)_c$. In particular, we arrive at the result that the constants B determined from the fits satisfy $|B| \lesssim 0.005$ and the magnitude of corresponding uncertainties are comparable with $|B|$. We consider these outcomes as a strong indication that our data of $\overline{T_N}/\overline{c}^{3/2}$, as a function of $\overline{M_s}$, can be described well by a linear function of $\overline{M_s}$ passing through the origin.

IV. DISCUSSIONS AND CONCLUSIONS

For clean 3D dimerized quantum Heisenberg models, it is established that the physical quantities $T_N/c^{3/2}$ and $T_N/\overline{J}$, as functions of M_s, scale linearly with M_s. Notice since three spatial dimensions is the upper critical dimensions associated with the related quantum phase transition, one expects there are logarithmic corrections to T_N and M_s close to the critical point. The linear scaling relations between T_N and M_s indicate that the exponents associated with the logarithmic corrections to T_N and M_s take the same values. This result is obtained theoretically in Refs. [39,40] and is confirmed in Ref. [41].

Motivated by these universal scaling relations between T_N and M_s for the clean 3D dimerized systems, here we study these relations for a 3D quantum Heisenberg model with configurational disorder. A remarkable result observed in our investigation is that close to the considered critical point, the relations $T_N/c^{3/2} = AM_s$ and $T_N\overline{J} = A_1M_s$ remain valid for the studied model with the introduced disorder. In addition, both the obtained data of $\overline{T_N}$ and $\overline{M_s}$ in this study do receive multiplicative logarithmic corrections and are fully compatible with the expected critical behavior for clean dimerized models. This indicates that the related quantum phase transition of the studied system may be described by the same critical theory as that of its clean analogues.

According to the Harris criterion and its generalization [54–56], if the correlation length exponent ν for a critical point of a clean quantum system satisfies the inequality $\nu D > 2$ (D is the spatial dimensionality), then with the presence of (quenched) disorder the resulting critical behavior remains the same. On the other hand, if the inequality $\nu D > 2$ is violated, then the associated phase transition of the model with (weak) spatial disorder must be governed by a new universality class so that the inequality $\nu D > 2$ is fulfilled, assuming that the new critical point is still well-defined. In addition to these two scenarios, there also exists a so-called infinite-randomness category for which the disordered systems usually show unconventional dynamical scaling [44].

With the Harris criterion, one may intuitively expect that the considered configurational disorder is relevant. This is because the related quantities of the clean analogues of the studied disordered model do not satisfy the inequality $\nu D > 2$. However, the results obtained here suggest that the Harris criterion is not valid for the 3D spin-1/2 dimerized Heisenberg model with configurational disorder.

While many studies of classical disordered systems are consistent with the scenarios given by the Harris criterion, the applicability of Harris criterion for dimerized quantum spin and Boson systems with the presence of disorder is less satisfactory. For example, studies of two-dimensional (2D) dimerized spin-1/2 Heisenberg model (on the square lattice) with certain kinds of bond disorder, including the close-packed and configurational disorder introduced in [45] and the dimer-type disorder employed in [57], indicate that the corresponding phase transitions are still governed by the critical theory for their clean counterparts, i.e., $O(3)$ universality class [45,57]. This demonstrates that besides the configurational disorder, the Harris criterion is not applicable for other kinds of disorder as well. Moreover, it is likely that when these mentioned types of disorder are present in the 3D systems, the resulting zero temperature phase transitions associated with dimerization will still belong to the mean-field universality class with multiplicative logarithmic corrections. In summary, although there are numerous studies regarding the Harris criterion, under which circumstances will it be valid is still not firmly established yet. Finally, we want to highlight the fact that the known dimerized quantum spin systems for which the Harris criterion is valid are the 2D Heisenberg models with random dimer-dilution [58–61]. As a result, it will be exciting to carry out studies of 3D spin-1/2 systems with random dimer dilution to examine whether the results obtained here remain true for these 3D bond-diluted models.

It is also interesting to understand the effects of disorder on the upper critical dimension D_c related to the considered phase transition, namely quantum phase transition triggered by dimerization for spin-1/2 Heisenberg models. For a disordered quantum spin system which has spatial dimensions equal to the D_c of clean dimerized spin-1/2 models (here $D_c = 3$), if the Harris criterion is valid, then the disorder increases the D_c of the system when it is compared to that of clean models. This conclusion is based on the facts that the condition $\nu D > 2$ must be fulfilled and the critical exponents are the ones of mean-field when D is above D_c. On the other hand, if the Harris criterion is violated, then the effects of disorder on the D_c of the studied system need further examination. For example, for the investigated model in our study, the D_c of the considered disordered system remains the same as the one of clean dimerized quantum spin models. This is because the obtained data can be fitted quantitatively to *Ansätze* of mean-field exponents with multiplicative logarithmic corrections. On the other hand, assuming that no logarithmic corrections

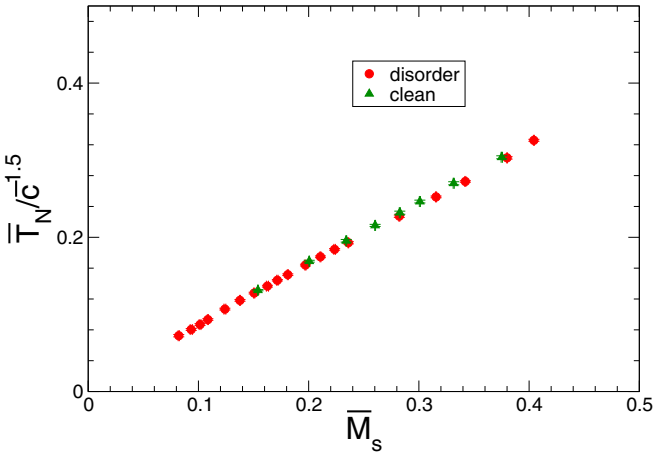

FIG. 16. $\overline{T_N}/\overline{c}^{3/2}$ as functions of $\overline{M}$ for both the considered disordered model in this investigation and the clean model studied in Ref. [35]. The $\overline{T_N}$ used in the figure for the disordered model are determined from the observable $\overline{Q_1}$.

are observed for a 3D dimerized spin-1/2 system with the presence of certain kind of disorder, and that its data can be understood well by the mean-field exponents, then clearly the D_c of this disordered system is below that of clean dimerized quantum spin models.

In Ref. [41], it is found that for the clean 3D double cubic quantum Heisenberg model the numerical value of the coefficient A in $T_N/c^{3/2} = AM_s$ is given by $A \sim 1.084$. For the disordered model considered here, the corresponding coefficient is given by $A \sim 0.86$, which is different from $A \sim 1.084$ associated with the double cubic model studied in Ref. [41]. Consequently, this coefficient A is likely not universal and depends on the microscopic details of the investigated systems. Interestingly, using the data determined here and that of a clean system calculated in Ref. [35], smooth universal curves associated with the studied scaling relations do show up (see Figs. 16 and 17). This implies

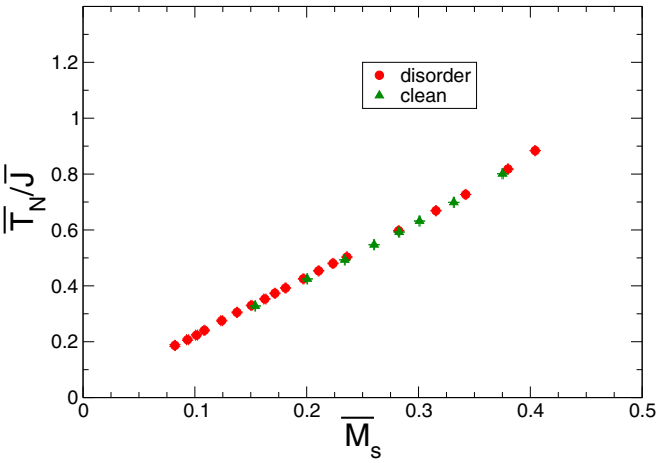

FIG. 17. $\overline{T_N}/\overline{J}$ as functions of $\overline{M}$ for both the considered disordered model in this investigation and the clean model studied in Ref. [35]. The $\overline{T_N}$ used in the figure for the disordered model are determined from the observable $\overline{Q_1}$.

that while not being generally true, universal coefficients may still exist within models sharing some similar characters. It will be interesting to investigate, in a more quantitative manner, that under what conditions will the coefficients A and A_1 of different models take the same numerical values. In particular, conducting similar investigation as the one presented here for the 3D dimerized quantum spin models with random dimer-dilution will be extremely compelling, since such studies not only serve as checks for the universal scaling shown in Figs. 16 and 17, the obtained results will also be useful in better understanding the Harris criterion.

Although based on our investigation we conclude that the coefficient A is likely not universal, we find the quantity $A/(J'/J)_c^{3/2}$ determined in this investigation matching very well with the corresponding result in Ref. [41]. Specifically, using the data available in Ref. [41] and here, we reach $A/(J'/J)_c^{3/2} \sim 0.1019$ and $A/(J'/J)_c^{3/2} \sim 0.1011$ for the double cubic model and the disordered model studied here, respectively. Notice the numerical values of $A/(J'/J)_c^{3/2}$ obtained from two different models are in very good agreement with each other. While our preliminary result of $A/(J'/J)_c^{3/2}$ of other dimerized model does not seem to support the scenario that the quantity $A/(J'/J)_c^{3/2}$ takes a universal value, the investigation carried out in this study suggests true universal quantities may still emerge for both the clean and disordered 3D antiferromagnets (which share some similar properties). Uncovering the possible hidden universal relations of 3D antiferromagnets will be an interesting topic to conduct in the future.

Besides being important and interesting from a theoretical perspective, the results obtained in this study are relevant to the experimental data of $TlCuCl_3$ as well. For example, the linear relations between $\overline{T_N}$ and $\overline{M_s}$ close to the critical point shown here are analogues to the one demonstrated in Ref. [36]. Furthermore, similar to the findings in Ref. [36] that no logarithmic corrections are observed, the $\overline{M_s}$ data calculated here show the same behavior, although with a different value for the exponent. We would like to point out that while the obtained data of $\overline{M_s}$ can be fitted to an *Ansatz* of the form $a_1|j_c - j|^{b_1}$, these data can also be understood well using the same *Ansatz* with a multiplicative logarithmic correction. It should also be highlighted that the $\overline{T_N}/\overline{J}$ data determined here can only be described quantitatively and systematically by the second *Ansatz* in Eq. (11). Finally, it is argued in Ref. [36] that while the quantum critical scaling relations are solely determined by the macroscopic properties of the underlying system, to compare these theoretical scaling predictions with the relevant experimental data requires the knowledge of nonuniversal prefactors. Indeed, without appropriate normalization, the prefactor A in the scaling relation $\overline{T_N}/\overline{c}^{3/2} = A\overline{M}$ determined here differs from the one obtained in Ref. [41]. In conclusion, studies of other 3D disordered and clean models may shed some light on clarifying whether true universal scaling relations do exist for 3D quantum antiferromagnets.

ACKNOWLEDGMENTS

We thank A. W. Sandvik for encouragement. This study is partially supported by Ministry of Science and Technology of Taiwan (Grant No. MOST 105-2112-M-003-002-MY3).

[1] N. Goldenfeld, *Lectures On Phase Transitions And The Renormalization Group (Frontiers in Physics)* (Addison-Wesley, Reading, MA, 1992).

[2] S. Sachdev, *Quantum Phase Transitions* (Cambridge University Press, Cambridge, 1999).

[3] L. D. Carr, Understanding Quantum Phase Transitions, *Condensed Matter Physics* (CRC Press, 2010).

[4] M. Matsumoto, C. Yasuda, S. Todo, and Hajime Takayama, Phys. Rev. B **65**, 014407 (2001).

[5] L. Wang, K. S. D. Beach, and A. W. Sandvik, Phys. Rev. B **73**, 014431 (2006).

[6] S. Wenzel, L. Bogacz, and W. Janke, Phys. Rev. Lett. **101**, 127202 (2008).

[7] A. F. Albuquerque, M. Troyer, and J. Oitmaa, Phys. Rev. B **78**, 132402 (2008).

[8] S. Wenzel and W. Janke, Phys. Rev. B **79**, 014410 (2009).

[9] F.-J. Jiang and U. Gerber, J. Stat. Mech. (2009) P09016.

[10] F.-J. Jiang, Phys. Rev. B **85**, 014414 (2012).

[11] M. Campostrini, M. Hasenbusch, A. Pelissetto, P. Rossi, and E. Vicari, Phys. Rev. B **65**, 144520 (2002).

[12] A. Pelissetto and E. Vicari, Phys. Rep. **368**, 549 (2002).

[13] L. Fritz, R. L. Doretto, S. Wessel, S. Wenzel, S. Burdin, and M. Vojta, Phys. Rev. B **83**, 174416 (2011).

[14] S. Chakravarty, B. I. Halperin, and D. R. Nelson, Phys. Rev. Lett. **60**, 1057 (1988).

[15] J. D. Reger and A. P. Young, Phys. Rev. B **37**, 5978(R) (1988).

[16] S. Chakravarty, B. I. Halperin, and D. R. Nelson, Phys. Rev. B **39**, 2344 (1989).

[17] H. Neuberger and T. Ziman, Phys. Rev. B **39**, 2608 (1989).

[18] P. Hasenfratz and H. Leutwyler, Nucl. Phys. B **343**, 241 (1990).

[19] P. Hasenfratz and F. Niedermayer, Phys. Lett. B **268**, 231 (1991).

[20] P. Hasenfratz and F. Niedermayer, Z. Phys. B **92**, 91 (1993).

[21] A. V. Chubukov, S. Sachdev, and J. Ye, Phys. Rev. B **49**, 11919 (1994).

[22] U.-J. Wiese and H.-P. Ying, Z. Phys. B **93**, 147 (1994).

[23] M. Troyer, H. Kontani, and K. Ueda, Phys. Rev. Lett. **76**, 3822 (1996).

[24] B. B. Beard and U.-J. Wiese, Phys. Rev. Lett. **77**, 5130 (1996).

[25] A. W. Sandvik, Phys. Rev. B **56**, 11678 (1997).

[26] F.-J. Jiang, F. Kampfer, M. Nyfeler, and U.-J. Wiese, Phys. Rev. B **78**, 214406 (2008).

[27] F.-J. Jiang, F. Kämpfer, and M. Nyfeler, Phys. Rev. B **80**, 033104 (2009).

[28] F.-J. Jiang and U.-J. Wiese, Phys. Rev. B **83**, 155120 (2011).

[29] N. Cavadini, G. Heigold, W. Henggeler, A. Furrer, H.-U. Güdel, K. Krämer, and H. Mutka, Phys. Rev. B **63**, 172414 (2001).

[30] Ch. Rüegg, N. Cavadini, A. Furrer, H.-U. Güdel, K. Krämer, H. Mutka, A. Wildes, K. Habicht, and P. Vorderwisch, Nature (London) **423**, 62 (2003).

[31] Ch. Rüegg, B. Normand, M. Matsumoto, A. Furrer, D. F. McMorrow, K. W. Krämer, H.-U. Güdel, S. N. Gvasaliya, H. Mutka, and M. Boehm, Phys. Rev. Lett. **100**, 205701 (2008).

[32] Y. Kulik and O. P. Sushkov, Phys. Rev. B **84**, 134418 (2011).

[33] J. Oitmaa, Y. Kulik, and O. P. Sushkov, Phys. Rev. B **85**, 144431 (2012).

[34] S. Jin and A. W. Sandvik, Phys. Rev. B **85**, 020409(R) (2012).

[35] M.-T. Kao and F.-J. Jiang, Eur. Phys. J. B **86**, 419 (2013).

[36] P. Merchant, B. Normand, K. W. Krämer, M. Boehm, D. F. McMorrow, and Ch. Rüegger, Nature Physics **10**, 373 (2014).

[37] D.-R. Tan and F.-J. Jiang, Eur. Phys. J. B **88**, 289 (2015).

[38] H. D. Scammell and O. P. Sushkov, Phys. Rev. B **95**, 024420 (2017).

[39] R. Kenna, Nucl. Phys. B **691**, 292 (2004).

[40] R. Kenna, *Order, Disorder and Criticality*, edited by Y. Holovatch (World Scientific, Singapore, 2012), Vol. 3, Chap. 1.

[41] Yan Q. Qin, B. Normand, A. W. Sandvik, and Z. Y. Meng, Phys. Rev. B **92**, 214401 (2015).

[42] H. Scammell and O. Sushkov, Phys. Rev. B **92**, 220401 (2015).

[43] O. P. Vajk, P. K. Mang, M. Greven, P. M. Gehring, and J. W. Lynn, Science **295**, 1691 (2002).

[44] T. Vojta, J. Low Temp. Phys. **161**, 299 (2010).

[45] D.-X. Yao, J. Gustafsson, E. W. Carlson, and A. W. Sandvik, Phys. Rev. B **82**, 172409 (2010).

[46] A. W. Sandvik, Phys. Rev. B **59**, R14157(R) (1999).

[47] A. W. Sandvik, Phys. Rev. B **66**, 024418 (2002).

[48] Here we will follow closely the introduction of β-doubling scheme in Ref. [47] and assume that the readers are familiar with SSE. We refer the readers who want to learn the elegant SSE algorithm to the relevant references [25,46].

[49] J. Cardy, *Scaling and Renormalization in Statistical Physics* (Cambridge University Press, Cambridge, 1996).

[50] In an early version of this manuscript, we claimed that for the J'/J close to $(J'/J)_c$, the corresponding values of $\overline{T_N}$ determined from $\overline{\rho_s}L$ deviate slightly from those associated with the Binder ratios. With higher-order *Ansätze*, careful investigation of deciding data range for the fits, and more statistics, now the discrepancies disappear for most of the considered J'/J. Consequently, some numerical analysis are redone and the corresponding results are updated. Conclusions remain the same.

[51] While it is likely that the determination of ν by considering the observable $\overline{\rho_s}L$ is affected by the presence of bond disorder, the quantitative agreement among the $\overline{T_N}$ obtained from $\overline{\rho_s}L$, $\overline{Q_1}$, and $\overline{Q_2}$ indicates that the calculated results of $\overline{T_N}$ are reliable.

[52] F.-J. Jiang, Phys. Rev. B **83**, 024419 (2011).

[53] A. Sen, H. Suwa, and A. W. Sandvik, Phys. Rev. B **92**, 195145 (2015).

[54] A. B. Harris, J. Phys. C **7**, 1671 (1974).

[55] J. T. Chayes, L. Chayes, D. S. Fisher, and T. Spencer, Phys. Rev. Lett. **57**, 2999 (1986).

[56] O. Motrunich, S. C. Mau, D. A. Huse, and D. S. Fisher, Phys. Rev. B **61**, 1160 (2000).

[57] N. Ma, A. W. Sandvik, and D.-X. Yao, Phys. Rev. B **90**, 104425 (2014).

[58] A. W. Sandvik, Phys. Rev. Lett. **89**, 177201 (2002).

[59] R. Yu, T. Roscilde, and S. Haas, Phys. Rev. Lett. **94**, 197204 (2005).

[60] R. Sknepnek, T. Vojta, and M. Vojta, Phys. Rev. Lett. **93**, 097201 (2004).

[61] A. W. Sandvik, Phys. Rev. Lett. **96**, 207201 (2006).